

Dielectric spectroscopy on two orientationally disordered crystals: NPA ($\text{CH}_2\text{OHC}(\text{CH}_3)_3$) and TCE ($\text{CH}_2\text{OHCCl}_3$)

This article has been downloaded from IOPscience. Please scroll down to see the full text article.

2000 J. Phys.: Condens. Matter 12 3871

(<http://iopscience.iop.org/0953-8984/12/16/309>)

View [the table of contents for this issue](#), or go to the [journal homepage](#) for more

Download details:

IP Address: 171.66.16.221

The article was downloaded on 16/05/2010 at 04:50

Please note that [terms and conditions apply](#).

Dielectric spectroscopy on two orientationally disordered crystals: NPA ($\text{CH}_2\text{OHC}(\text{CH}_3)_3$) and TCE ($\text{CH}_2\text{OHCCl}_3$)

D O López[†]§, J Ll Tamarit[†], M R de la Fuente[‡], M A Pérez-Jubindo[‡],
J Salud[†] and M Barrio[†]

[†] Departament de Física i Enginyeria Nuclear, ETSEIB, Universitat Politècnica de Catalunya,
Diagonal 647, 08028 Barcelona, Spain

[‡] Departamento de Física Aplicada II, Facultad de Ciencias, Universidad del País Vasco,
Apartado 644, E-48080 Bilbao, Spain

E-mail: david.orencio.lopez@upc.es

Received 14 January 2000, in final form 16 February 2000

Abstract. The dielectric relaxation spectra of NPA ($\text{CH}_2\text{OHC}(\text{CH}_3)_3$) and TCE ($\text{CH}_2\text{OHCCl}_3$) have been determined in the orientationally disordered state (ODIC) and for TCE also in the liquid state. The studied temperature ranges have been 313–233 K and 293–255 K for NPA and TCE respectively. The frequency dependence of the complex dielectric permittivity is well described in both cases by the Cole–Davidson function. From the fits to this equation, dielectric strengths, relaxation times and spectral shape parameters as functions of temperature have been obtained. The relaxation times are thermally activated following an Arrhenius law for NPA and a Vogel–Fulcher–Tammann law for TCE. Likewise, for NPA a new intermediate ODIC state has been stated by means of dielectric and x-ray diffraction measurements.

1. Introduction

A certain group of molecular substances (organic or not) composed of globular or pseudo-globular molecules often give rise to a *mesophase* or *mesostate* between the isotropic liquid and ‘ordered’ crystalline state. In such a mesostate, the molecules have rotational freedom and are disposed in a rather symmetrical lattice, generally either cubic or rhombohedral. This mesostate is often referred to as the plastic crystalline state and the molecular substances are known as plastic crystals or orientationally disordered crystals (ODICs for short). The transition from ODIC state to liquid is characterized by small changes in volume and entropy. Some examples of such ODIC substances are the well known neopentane ($\text{C}(\text{CH}_3)_4$) and carbon tetrachloride (CCl_4).

The aim of this work is to perform a dielectric study on two ODIC materials: neopentylalcohol (NPA, ($\text{CH}_2\text{OHC}(\text{CH}_3)_3$)) and 2,2,2-trichloroethanol (TCE, $\text{CH}_2\text{OHCCl}_3$). Both compounds have similar molecular geometry, with a unique ($-\text{CH}_2\text{OH}$) group and therefore, from the point of view of intermolecular interactions, one might expect a similar hydrogen bonding scheme. Likewise, it may be underlined that the chlorine atom has practically the same volume as the methyl group. Up to date, experimental dielectric studies on tetrahedral molecular compounds closely related to the above-mentioned are rather scarce [1–4]. The fundamental reason for this fact is probably a relatively high frequency domain for the dielectric losses. One advantage of the compounds studied in this work in relation to other with

§ Author to whom correspondence should be addressed.

similar shape and size must be evidenced. A very simple change in the molecular configuration, as the introduction of a group with the ability to generate hydrogen bonds, enables us to maintain the 'structural isotropy' (lattices remain in the cubic system) and, at the same time, to produce strong changes on the intermolecular interactions. Thanks to them, the characteristic relaxation time of the molecular tumbling considerably decreases without losing the orientational disorder. Moreover, the fact that the relaxation time decreases in comparison with other spherical molecules enables the analysis of both liquid and ODIC phases. So then, the influence of the disappearance of the translational degrees of freedom when the substances freeze makes it possible to compare close molecular surroundings in a different long-range order scheme.

As far as NPA is concerned, differential thermal analysis by DSC [3, 5], NMR [6], x-ray powder diffraction [5, 7–9], static dielectric permittivity at normal pressure and complex permittivity under pressure [3] have been studied in the last 30 years, making evident its particular polymorphism. The existence of two stable and structurally different solid forms has been established: a low-temperature ordered state (form II) which recently has been determined to be triclinic [9]—stable up to 235.4 K—and an ODIC state (form I), the structure of which is face centred cubic (probably $Fm\bar{3}m$) [7]—stable up to the melting point at 329.8 K. Nevertheless, Würflinger and co-workers in a relatively recent study of differential thermal analysis (DTA) and dielectric spectroscopy under pressure, showed the possible existence of two ODIC states. The transition between them was observable in the static permittivity measurements but not in the DTA measurements [3]. On the other hand, a recent x-ray powder diffraction study [5] has shown the next behaviour. Once NPA in its ODIC state is cooled fast enough to prevent the transition I–II, the ODIC state is supercooled and finally a glassy state is formed, the glass transition temperature being about 123 K. A glassy state can be defined as a state out of equilibrium in which the orientational disorder has been partially frozen, keeping the lattice symmetry of the ODIC state. To date, no heat capacity data concerning the glass transition of the NPA pure compound have been published.

As far as TCE is concerned, and despite the molecular structural analogies with NPA, so far only one work has been reported in the literature about the phase behaviour of TCE at normal pressure and under pressure [10]. In such a work, the P – T and P – v – T phase diagrams were reported in order to determine the phase properties and specific volumes for the liquid and solid states. In spite of the complexity of the phase diagram, at normal pressure there exists, at least, a stable solid form (II)—stable up to the melting temperature at 290.6 K—and a metastable ODIC state (I) which has a monotropic nature—on cooling from the liquid state it undergoes a phase transition at 269.4 K which melts at 271.6 K. On the other hand, to date there is no evidence for the existence of a possible glass and/or glassy state.

The paper is organized as follows. In section 2 we describe the experimental details both for dielectric and x-ray powder diffraction measurements. In section 3, a presentation of the results along with a discussion will be given. The results will be compared with others previously published when possible and with other related compounds. From the fragility parameter, the studied compounds will be classified as glasslike formers and from the Kirkwood g factor, information about their dipolar arrangements will be given. Finally, in section 4, a summary of the main conclusions will be made.

2. Experiment

2.1. Materials

NPA and TCE were obtained from Aldrich Chemical Company with purities of 99% and 99%+ respectively. Additional purification was performed using some standard methods [5, 9]. The results were controlled by means of differential scanning calorimetry (DSC).

2.2. Dielectric measurements

The measurements of complex dielectric permittivity were performed with two different impedance analysers: the HP4191A for the 10^6 – 10^9 Hz range and the HP4192A for the 10^2 – 10^6 Hz range. The former measures the impedance of the sample from the reflection coefficient at the end of a $50\ \Omega$ co-axial transmission line. Thus, the cell consists of two gold-plated brass electrodes (diameter 5 mm) separated by two $50\ \mu\text{m}$ thick silica spacers making a plane capacitor located at the end of the line. We used as sample holder a modified HP16091A co-axial test fixture. This was adapted by a connector, which allows us to go from APC7 to four wires in order to perform measurements with the low frequency analyser. The sample holder was held in a cryostat, which screens the system, and both temperature and dielectric measurements were fully computer controlled [11, 12].

In order to perform the dielectric measurements, the materials were heated up to their liquid states and introduced into the dielectric cell. Likewise, to prevent the possibility of hole formation in the inter-electrode space an additional mechanical device was used. A test of the sample capacity was also made before the measurements. These were made in similar conditions, on slow cooling and stabilization at different temperature steps (± 0.2 K). The data for NPA were collected from 313 to 233 K every 5 K in the ODIC state. At temperatures higher than 313 K, the measurements were not successful owing to the high frequency of the dielectric loss. At temperatures lower than 233 K, NPA undergoes a phase transition to the solid ordered state (II) and all attempts to supercool it were unsuccessful. As for TCE, the data were collected from 293 to 255 K every 2 K in liquid and ODIC states. At temperatures lower than 255 K, TCE transforms to the solid ordered state (II).

2.3. X-ray powder diffraction measurements

The x-ray powder diffraction measurements were performed with a horizontally mounted INEL cylindrical position-sensitive detector (CPS-120) [13] equipped with a liquid-nitrogen INEL CRY950 cryostat (80–330 K). The detector, with a radius of curvature of 250 mm, used in Debye–Scherrer geometry, consisted of 4096 channels and the angular step was around 0.03° in 2θ -Bragg angle. Monochromator Cu $K\alpha_1$ radiation ($\lambda = 1.5406\ \text{\AA}$) was selected with an asymmetric focusing incident-beam curved quartz monochromator. The generator power was set at 40 kV and 30 mA. The powder samples were introduced in 0.5 mm Lindemann glass capillaries which rotate during the experiment to improve averaging of the crystallites.

External calibration using the cubic phase $\text{Na}_2\text{Ca}_3\text{Al}_2\text{F}_4$ was performed to convert channels to $^\circ (2\theta)$ by means of cubic spline fittings in order to correct the deviation from angular linearity in PSD according to recommendations [14, 15]. Diffractinel software was used for the calibration and for the peak position determinations after Gaussian fittings in the standard measurements.

A set of powder diffractograms was obtained in the ODIC state of NPA (233–323 K) at every 2 K step in the temperature range between 263 K and 283 K and at every 10 K step out of this range. The acquisition times were 60 min. The slew rate was $1\ \text{K min}^{-1}$ with stabilization time of 10 min at each temperature before data acquisition.

3. Results and discussion

3.1. The static permittivity

Figure 1 presents the static permittivity ϵ_s as a function of temperature both for NPA and TCE. Likewise, for NPA, some normal pressure permittivities from Würflinger and co-workers [3]

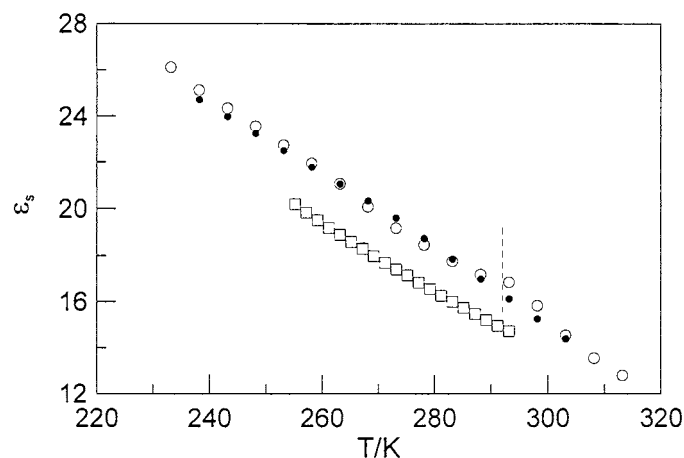


Figure 1. The static permittivity (ϵ_s) as a function of temperature for NPA (\circ) in ODIC state and TCE (\square) in ODIC and liquid states. (\bullet) Values from [3].

are also plotted, showing good agreement with our data. From such a figure it is not possible to observe the liquid–ODIC transition in TCE. Nevertheless we observe a slight change in the evolution of the static permittivity for NPA at around 290 K. So, in order to elucidate the existence of the non-observed transition (for TCE) and the observed anomaly (for NPA), the dielectric strength ($\Delta\epsilon = \epsilon_s - \epsilon_\infty$; ϵ_∞ is the permittivity at high frequency) and inverse temperature values are plotted against one another, see figure 2. According to Onsager theory [16], dipoles free to rotate should result in the relaxation strength being proportional to $1/T$. In such a figure, we clearly observe two different slopes whatever the compound is, making evident the existence of phase transitions. As for TCE, that corresponds to the L–ODIC transition being ~ 273 K. As for NPA the phase transition takes place at about 290 K. Such a transition was postulated eight years ago by Würflinger *et al* as a possible intermediate transition between two ODIC states. This was visible as a slight change in static permittivity evolution with temperature at several pressures. Likewise, it was also visible in a DSC study but not observed in the DTA study [3]. In order to confirm its existence, a x-ray powder diffraction study has been performed. Figure 3 depicts the molar volume—calculated using the cubic lattice parameter—for the ODIC state along with the volume expansivity both as a function of temperature. In spite of the continuous evolution of the molar volume with temperature, a change in the expansivity is found at ~ 290 K, which is known to be an indication of a second-order transition. To sum up, the existence of two ODIC states, ODIC(I) the plastic state just below the liquid state and ODIC(II) the plastic state just above the monoclinic solid, have been conclusively established. It must be pointed out that in a previous x-ray diffraction study [9] this transition was not detected probably due to the large temperature steps of the measurements.

3.2. The dynamic permittivity

Figures 4 and 5 show tridimensional plots of the dielectric losses ϵ'' versus temperature and frequency for both compounds NPA and TCE, respectively. The contribution of DC conductivity to the response, which is mainly due to the hydrogen bond effects, has been previously subtracted. These figures clearly show only one relaxation process in the measured range, whatever the phase (liquid and ODIC) and compound is, related to the flip–flop of the

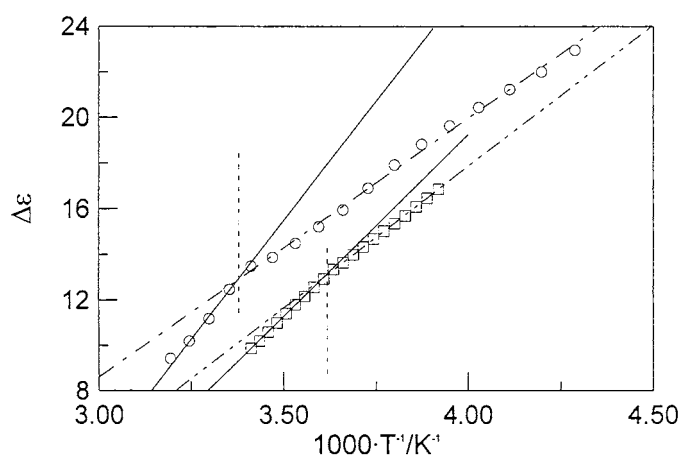


Figure 2. The dielectric strength ($\Delta\varepsilon$) as a function of inverse temperature for NPA (O) and TCE (□).

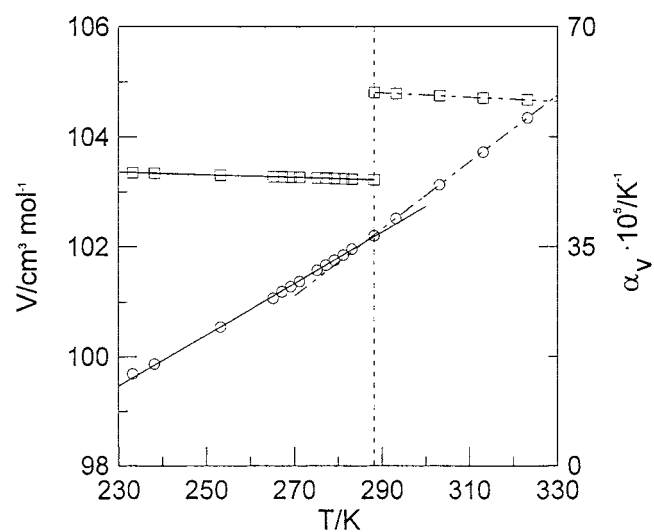


Figure 3. Molar volume (O) and volume expansivity (□) for ODIC state against temperature for NPA.

molecular dipoles. A possibly secondary relaxation process, which in the present case could be associated with the internal rotation, did not appear in the measured frequency range providing an additional facility to analyse the primary α -relaxation.

The results of the complex permittivity were fitted to the Havriliak–Negami (HN) [17] equation

$$\varepsilon(\omega) = \varepsilon_{\infty} + \left[\frac{\Delta\varepsilon}{(1 + (i\omega\tau)^{\alpha})^{\beta}} \right] \quad (1)$$

where $\varepsilon(\omega)$ is the complex permittivity ($\varepsilon(\omega) = \varepsilon'(\omega) - i\varepsilon''(\omega)$), $\Delta\varepsilon$ stands for the dielectric strength ($\varepsilon_s - \varepsilon_{\infty}$), α and β parameters determine the spectral shape and τ is the relaxation

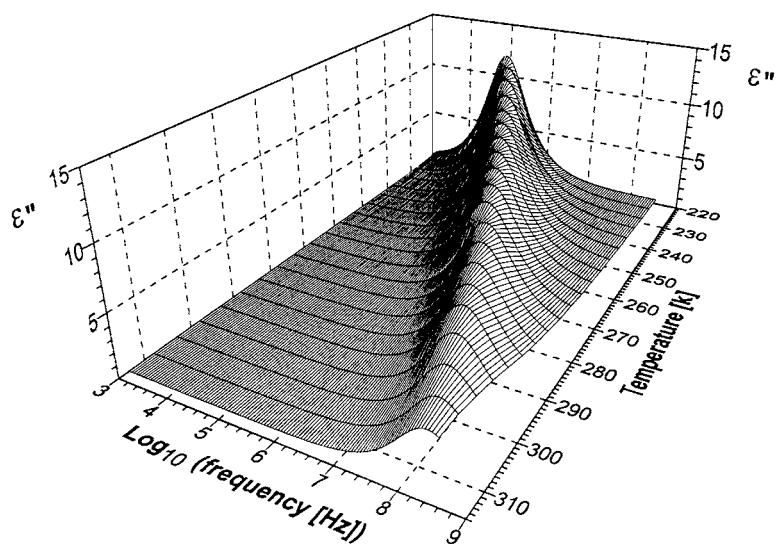


Figure 4. Dielectric losses against temperature and frequency for NPA.

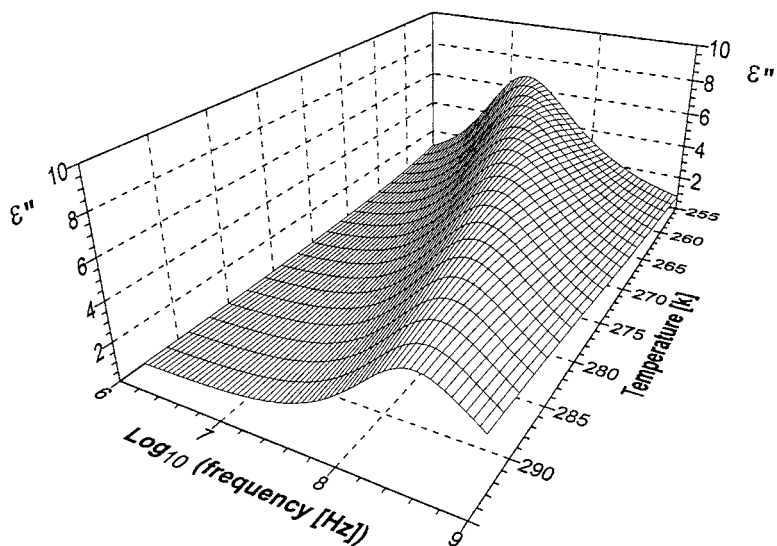


Figure 5. Dielectric losses against temperature and frequency for TCE.

time which is related to the frequency of maximum losses through

$$\tau = \frac{1}{2\pi f} \left[\tan \left(\frac{\pi}{2(\beta + 1)} \right) \right]^{1/\alpha} \quad (2)$$

The adjustable parameters α , β , τ and ε_{∞} were simultaneously determined in a fitting procedure of equation (1). Figure 6 shows ε'' against the logarithm of the frequency at certain temperatures together with HN fits.

For both compounds α was determined to be the unity whatever the phase is and consequently the dielectric relaxation is well described by means of the Cole–Davidson

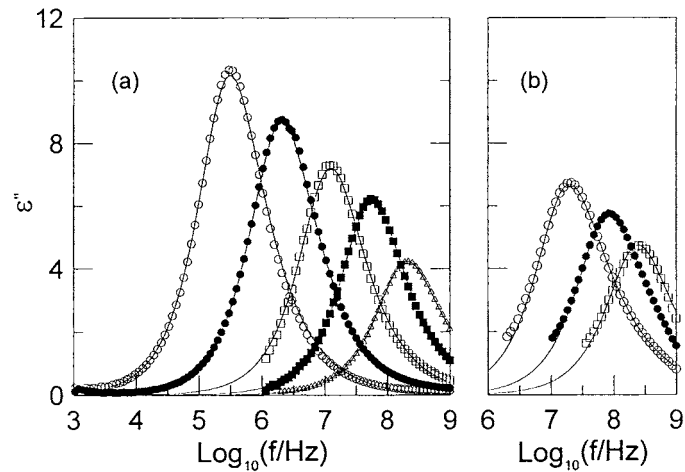


Figure 6. Imaginary ϵ'' part of the dielectric permittivity for various selected temperatures for (a) NPA at (○) 233 K, (●) 253 K, (□) 273 K, (■) 293 K, (△) 313 K, and for (b) TCE at (○) 257 K, (●) 273 K, (□) 289 K. Solid lines correspond to Havriliak–Negami fits.

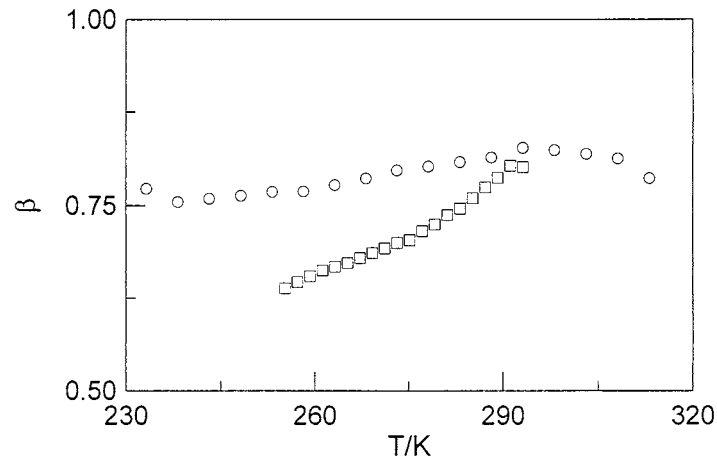


Figure 7. The dependence of the width parameter β on temperature for NPA (○) and TCE (□).

function [18], like other related compounds [4, 19]. Figure 7 shows the width parameter β as a function of temperature for both compounds. Such a parameter measures the degree of departure from Debye relaxation ($\beta = 1$). It seems to be evident that such a departure is practically constant for NPA in the studied temperature range. In contrast, the TCE relaxation behaviour moves increasingly away from the Debye behaviour when temperature decreases.

3.3. Relaxation times

Figure 8(a) shows, in an Arrhenius plot, the relaxation time τ versus inverse temperature for NPA and TCE. As for NPA it seems to be possible to describe the dependence of the relaxation time by an Arrhenius law (equation (3)), whatever the ODIC phase is:

$$\tau = \tau_0 \exp(A/T). \quad (3)$$

In such an equation, A accounts for the activation enthalpy $\Delta H (= AR)$ where R is the gas constant and τ_0 is a pre-exponential factor that represents a characteristic time of the order of atomic oscillations. The activation enthalpy of NPA, for both ODIC states, together with that reported by Würflinger and co-workers [3] is given in table 1. It may be emphasized that such values are rather similar. In order to compare with related molecular compounds, the activation enthalpy values of NPG ($\text{CH}_3)_2\text{C}(\text{CH}_2\text{OH})_2$) and TRIS compounds ($\text{CH}_3\text{NH}_2\text{C}(\text{CH}_2\text{OH})_3$) previously published [4] are also included in table 1. It is known that high activation enthalpies are indicative of a high degree of intermolecular association, due to strong intermolecular interactions. Nevertheless, the value for NPG is slightly lower than for NPA, despite the existence of a higher number of hydroxyl groups, and so the possibility of formation of a higher number of hydrogen bonds. In order to reconcile this observation, a more accurate revision of the published NPG values has been made. Figure 8(b) displays the values of NPG showing non-Arrhenius behaviour despite the short analysed temperature range and, therefore, we cannot calculate the activation enthalpy by means of an Arrhenius law. On the other hand, TRIS compound presents the highest value of activation enthalpy from among those reported in table 1. This fact would not be surprising, taking into account that the possibility of formation of hydrogen bonds is greater than for NPA and NPG.

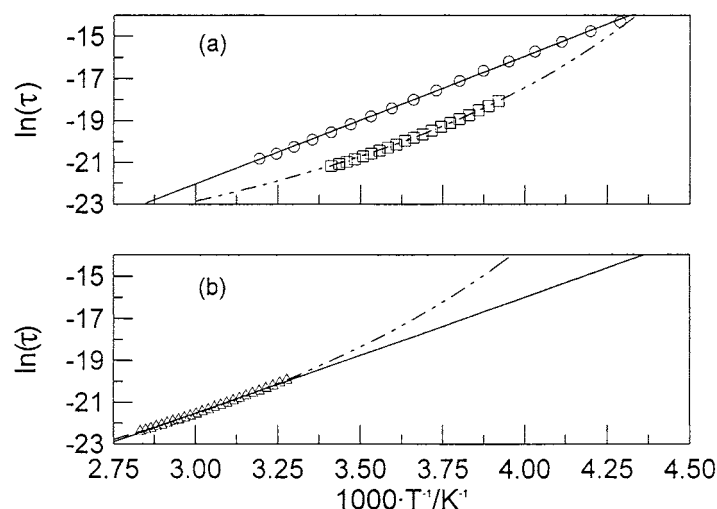


Figure 8. Arrhenius plot of the relaxation time τ . (a) NPA (\circ) and TCE (\square). (b) NPG (\triangle). Solid lines are fittings to the Arrhenius law. Dot-dashed lines are fittings to VFT law.

A more exhaustive revision of the values of activation enthalpies for the ODIC state of alicyclic alcohols, like cyclopentanol, cyclohexanol, cycloheptanol [19–24] and other branched alcohols like neohexanol, neoctanol, . . . [3, 24] has been made. It seems that the enthalpy of activation does not strongly depend on the nature of the alcohol. We would find it difficult to reconcile these facts with a relaxation mechanism that depends in any specific manner on the existence of a hydrogen-bonded network.

As far as TCE is concerned, the relaxation time dependence on temperature seems to show a clear non-Arrhenius behaviour, in spite of the reduced analysed range. This behaviour is rather similar to that observed for the NPG compound, see figures 8(a) and 8(b). Such dependences are quite well described by the Vogel–Fulcher–Tamann (VFT) law [25] given by equation (4),

$$\tau = \tau_0 \exp(A/(T - T_0)) \quad (4)$$

Table 1. Parameters obtained from the fits of the temperature dependence of the relaxation time to the Arrhenius and Vogel–Fulcher–Tammann (VFT) equations.

Compound	Type of fit	Form	A (K)	T_0 (K)
NPA	Arrhenius	ODIC (I)	5987 (± 132)	—
	Arrhenius	ODIC(II)	6003 (± 67)	—
	Arrhenius	ODIC(II) ^a	5641	—
TCE	VFT	ODIC	859 (± 120)	169.6(± 6)
	VFT	ODIC+liquid	1009 (± 62)	161.9(± 3)
NPG	Arrhenius	ODIC	5521 ^b	—
	VFT	ODIC	1320 (± 54)	167.2(± 3)
TRIS	Arrhenius	ODIC	8070 ^c	—

^a Value from [3].^b Fitting from values [4].^c Supercooled state. Value from [4].

where τ_0 is a pre-exponential factor. T_0 is the Vogel temperature and A is a parameter with dimension of temperature. The fitting parameters corresponding to the VFT law are also included in table 1.

The VFT law is habitually used for the glass state where the disorder of the liquid state (or the orientational disorder of the ODIC state) has been partially frozen, that shows a non-Arrhenius behaviour typical of molecular processes when approaching a glass transition. The Vogel temperature is also considered as the *ideal glass transition temperature*, 30 to 50 K below the calorimetric glass transition T_g . Such a temperature, which appears to be closely related to the freezing of well defined large-amplitude motions, takes place when the relaxation time reaches 10^2 s.

As for TCE, the calculated T_g from equation (4) is 196 K—taking into account the fit only for the ODIC state—or 192 K—adopting a unique fit for both liquid and ODIC states. Unfortunately, nowadays there is no experimental evidences about T_g .

As far as the T_g of NPA is concerned, the calculated value from equation (3) is 134.7 K—taking into account ODIC(II) state. The calorimetric value linearly extrapolated from data of the experimental phase diagram NPA+NPG [5] is 130.9 K. It is important to realize that T_g evolves almost linearly with mole fraction for normal alcohols [27]. The value reported by means of the x-ray diffraction technique is slightly lower than the former (≈ 123 K).

As for NPG, the calculated T_g from equation (4) is 205.7 K. The calorimetric value [5] obtained using the same method as for NPA is about 225 K. It may be underlined that x-ray diffraction data about the glass transition are not available to date.

On the other hand, the glass-like-formers can be classified taking into account the fragility parameter m [26], given by

$$m = \left[\frac{d \lg \tau}{d(T_g/T)} \right]_{T=T_g}. \quad (5)$$

We obtained $m = 21$ for NPA and $m = 106$ for TCE. Likewise, the calculated parameter m of NPG according to the values from [4] is 79. From an inspection of other glass-like-formers [26], the most convincing conclusion we can establish is that the more fragile is the material the less Arrhenius is the temperature dependence of the relaxation time. In this context, we have to be then cautious when comparing values of activation enthalpy, because in a non-Arrhenius description, the A parameter is not related to the activation enthalpy.

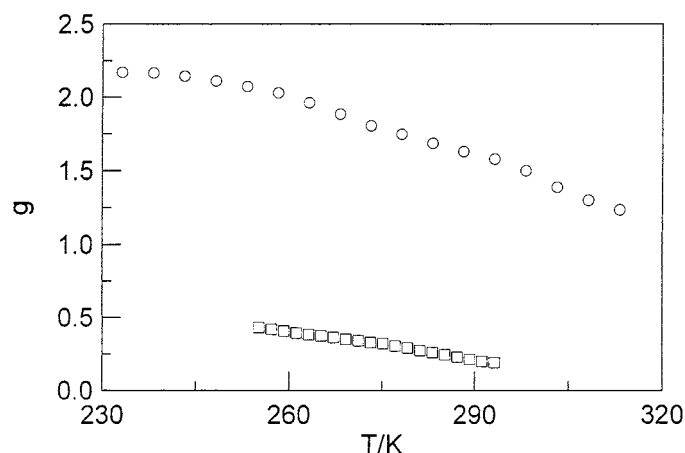


Figure 9. The Kirkwood- g factor dependence on temperature for NPA (○) and TCE (□).

On the other hand, a phenomenological relationship between the fragility m and the β -width parameter was proposed few years ago by Böhmer and co-workers [28]:

$$m = 250 - 320\beta^{KWW}(T_g) \quad (6)$$

where $\beta^{KWW}(T_g)$ is the width parameter at T_g of the relaxation process when described by means of the Kohlraush–Williams–Watts (KWW) function [29] instead of the Havriliak–Negami formula (equation (1)). A very simple relationship has been established between both β^{KWW} and β^{HN} ($\beta^{KWW} = (\beta^{HN})^{1/1.23}$) [30]. Equation (6) is qualitatively correct for pure materials but it must be taken cautiously when the temperature range of the dielectric spectrum analysed is far away from the glass transition temperature. In order to estimate m from equation (6), a linear extrapolation at T_g of β^{HN} in the ODIC state for both NPA and TCE has been made. The obtained values of m were 30 and 82, respectively. In spite of the arbitrariness of such extrapolations, the m value for NPA is rather close to that calculated by means of equation (5) in contrast to the value of TCE. Again, the explanation must be addressed to the non-Arrhenius behaviour of TCE that implies a clear non-linear evolution of β with temperature when approaching T_g . It must be pointed out that the non-linear effects increase when the temperature approaches the glass temperature. A direct observation of the analysed temperature range as a function of the reduced T_g/T temperature clearly shows that for TCE the lowest value corresponds to 0.75 while for NPA it is 0.58. Then the effects associated to the closeness of the non-ergodic state must be more relevant for TCE than for NPA.

3.4. Kirkwood's g factor

The correlation factor g , taking into account the Kirkwood–Frölich–Onsager theory [31], can be expressed by

$$g = \frac{9k_B T \varepsilon_0 V_m (\varepsilon_s - \varepsilon_\infty)(2\varepsilon_s + \varepsilon_\infty)}{\varepsilon_s (\varepsilon_\infty + 2)^2 N_A \mu^2} \quad (7)$$

in which V_m is the molar volume, k_B is the Boltzmann constant, N_A Avogadro's number and μ the dipole moment in the gas phase. The g factor, firstly introduced by Kirkwood, is a measure of short-range intermolecular forces that lead to specific dipole–dipole orientations.

In the absence of such forces, $g = 1$. According to the theory, g values larger than unity are interpreted as being due to a predominantly parallel alignment of neighbouring dipoles while g values smaller than unity correspond to an anti-parallel alignment.

Figure 9 shows the g factor evolution versus temperature for NPA and TCE. NPA presents g values larger than unity for the whole temperature range. This is a typical value in chain [32, 33], alicyclic [19–23] and branched [3, 24] alcohols indicating a preferred parallel correlation of the dipoles. However, for TCE, the g values are always lower than 0.5. It is quite unexpected that two close molecular shape compounds display a completely different short-range order. Such a result enables us to analyse the influence of dipolar interactions and the geometrical induced short-range order (i.e. steric factors). The dipolar moments of TCE and NPA (3.4 D and 1.8 D) are strongly different. Moreover, a straightforward calculation of the van der Waals volume of the molecules provides a volume for TCE about 7 \AA^3 lower than for NPA that by means of the density values produces a packing coefficient slightly higher for TCE. Such an experimental fact means that strong short-range correlations in the re-orientational disorder must be present in the case of TCE. This conclusion is reinforced by the value of Kirkwood g factor, which is a measure of the local ordering, being in the case of TCE anti-parallel. To end with, it is quite evident that the whole set of conditions appearing for the molecular relaxation of TCE gives rise to a lower local freedom producing a more complicated short-range order. Such a decrease of the dipolar local freedom is accounts for the lower value of β for TCE, which means a distance effect from Debye behaviour.

4. Conclusions

The study dealt with in this paper has provided the following main conclusions:

- (1) For the NPA compound, by means of dielectric spectroscopy and x-ray powder diffraction, we have established with no doubt the existence of two ODIC forms with identical lattice structures and very close dynamical properties.
- (2) For NPA and TCE compounds, the dielectric losses have been interpreted by means of the Havriliak–Negami equation, enhancing a non-Debye relaxation. The spectral α -parameter has been determined to be unity (Cole–Davidson) whereas the width β -parameter has been determined to be practically temperature non-dependent for NPA and decreasing with temperature for TCE.
- (3) The relaxation map clearly has shown two different behaviours. For NPA, the relaxation time obeys an Arrhenius law in contrast to TCE and a related compound (NPG) that follow a Vogel–Fulcher–Tammann law.
- (4) Within the strong/fragility classification of Angell, a non-Arrhenius behaviour of glass-like-formers is a direct consequence of the fragility of the material.
- (5) The study of both compounds (NPA and TCE) in terms of the Kirkwood g factor has provided information about the molecular dipolar arrangements. For NPA a parallel correlation is preferred in contrast to TCE.

Acknowledgments

The authors are grateful to the DGES (PB95-0032) and CICYT (MAT97-0986-C02-02) for financial support.

References

- [1] Chan R K and Johari G P 1974 *Annu. Rep. Conf. Electr. Insul. Dielectr. Phenom.* **43** 331
- [2] Danhauser W, Bahe L W, Lin R Y and Flueckinger A F 1965 *J. Chem. Phys.* **43** 257
- [3] Kreul H G, Waldinger R and Würflinger A 1992 *Z. Naturforsch.* a **47** 1127
- [4] Tamarit J Ll, Pérez-Jubindo M A and de la Fuente M R 1997 *J. Phys.: Condens. Matter* **9** 5469
- [5] Salud J, López D O, Barrio M and Tamarit J Ll 1999 *J. Mater. Chem.* **9** 909
- [6] Faucher J A, Graham J D, Koleske J V, Sante E R and Walter E R 1966 *J. Phys. Chem.* **70** 3778
- [7] Carpenter G B 1969 *Acta Crystallogr. B* **25** 163
- [8] Suenaga K, Kanae R, Matsuo T and Suga H 1990 *Proc. 11th IUPAC Conf. (Como)*
- [9] Salud J, Barrio M, López D O, Tamarit J Ll and Alcobé X 1998 *J. Appl. Crystallogr.* **31** 748
- [10] Jenau M, Sandmann M, Würflinger A and Tamarit J Ll 1997 *Z. Naturf. a* **52** 493
- [11] de la Fuente M R, Pérez-Jubindo M A, Zubia J, Pérez-Iglesias T and Seoane A 1994 *Liq. Cryst.* **16** 1501
- [12] de la Fuente M R, Merino S, Pérez-Jubindo M A and Sierra M T 1995 *Mol. Cryst. Liq. Cryst.* **259** 1
- [13] Ballon J, Comparat V and Pouxé J 1983 *Nucl. Instrum. Methods* **217** 213
- [14] Deniard P, Evain M, Barbet J M and Brec R 1991 *Mater. Sci. Forum* **79–82** 363
- [15] Evain M, Deniard P, Jouanneaux A and Brec R 1993 *J. Appl. Crystallogr.* **26** 563
- [16] Frölich H 1949 *Theory of Dielectrics* (London: Oxford University Press)
- [17] Havriliak S and Negami S 1966 *J. Polym. Sci. Polym. Symp.* **14** 89
- [18] Davidson D W and Cole R H 1950 *J. Chem. Phys.* **18** 1417
- [19] Würflinger A 1991 *Ber. Bunsenges. Phys. Chem.* **95** 1040
- [20] Poser U, Shulte L and Würflinger A 1985 *Ber. Bunsenges. Phys. Chem.* **89** 1275
- [21] Pingel N, Poser U and Würflinger A 1984 *J. Chem. Soc. Faraday Trans.* **80** 3221
- [22] Poser U and Würflinger A 1988 *Ber. Bunsenges. Phys. Chem.* **92** 765
- [23] Würflinger A 1982 *Ber. Bunsenges. Phys. Chem.* **86** 172
- [24] Edelman R, Bardelmeier U and Würflinger A 1991 *J. Chem. Soc. Faraday Trans.* **87** 1149
- [25] Vogel H 1961 *Z. Phys.* **22** 645
- Fulcher G S 1925 *J. Amer. Ceram. Soc.* **8** 339
- Tammann G and Hesse W 1926 *Z. Anorg. Chem.* **156** 2451
- [26] Lsikar A V 1977 *J. Solution Chem.* **6** 81
- [27] Angell C A 1991 *J. Non-Cryst. Solids* **131–133** 13
- [28] Böhmer R, Nagai K L, Angell C A and Plazek D J 1993 *J. Chem. Phys.* **99** 4201
- [29] Kohlrausch R 1854 *Prog. Ann. Phys.* **91** 179
- Williams G and Watts D C 1970 *Trans. Faraday Soc.* **66** 80
- [30] Alegria A, Guerrica-Echevarria E, Goitiandia L, Telleria L and Colmenero J 1995 *Macromol.* **28** 1516
- [31] Böttcher C J F and Bordewijk P 1978 *Theory of Electric Polarization* (Amsterdam: Elsevier)
- [32] Johari G P and Danhauser W 1968 *J. Chem. Phys.* **48** 5114
- [33] Vij J K, Scaife W G and Calderwood J H 1981 *J. Phys. D: Appl. Phys.* **14** 733